

Calibration of UWB UAV Radar for the Remote Measurement of Reflection Coefficient

Konstantin Muzalevskiy

Laboratory of Radiophysics of the
Earth Remote Sensing
Kirensky Institute of Physics Federal
Research Center KSC Siberian Branch
Russian Academy of Science
Krasnoyarsk, The Russian Federation
email: rsdkm@ksc.krasn.ru

Mikhail Mikhaylov

Laboratory of Radiophysics of the
Earth Remote Sensing
Kirensky Institute of Physics Federal
Research Center KSC Siberian Branch
Russian Academy of Science
Krasnoyarsk, The Russian Federation
email: fractaloff@mail.ru

Zdenek Ruzicka

Laboratory of Radiophysics of the
Earth Remote Sensing
Kirensky Institute of Physics Federal
Research Center KSC Siberian Branch
Russian Academy of Science
Krasnoyarsk, The Russian Federation
email: rsdzr@ksc.krasn.ru

Abstract—In this work, the possibility of the remote measurement of reflection coefficient in the ultra-wide frequency range from 425 MHz to 1010 MHz from the board of unmanned aerial vehicle (UAV) using ultra-wide band (UWB) radar was investigated. With this in mind, the antenna-feeder path of UAV UWB radar is calibrated. The calibration process consisted in measuring the reflection coefficient from the brass mesh sheet at various UAV hovering heights. Printed log-periodic dipole antenna was used as transmitter-receiver antenna. As a result, the antenna return loss in an empty-room and the complex antenna response function of the antenna-feeder path of the UAV UWB radar were found. It is shown that the amplitude of the reflected wave from a brass mesh sheet can be measured with root-mean square error (RMSE), $RMSE=0.017$ 1/m and a determination coefficient (R^2) of $R^2=0.967$. Therewith the UAV hovering heights measured by the pulse method and the on-board laser rangefinder correlates with each other with $R^2=0.999$ and with $RMSE=3.5$ cm (distance measurement error of the laser rangefinder is ± 1 cm, surface irregularities of the brass mesh sheet were no more than 1.5cm). Measured in the frequency range from 500 MHz to 900 MHz, the reflection coefficient from fresh lake water by UAV UWB radar with a relative error of no more than 7.5% (practically does not depend on the height of the UAV hovering, approximately from 2.2 m to 5.2 m) coincides with the calculated one by the Stogryn's formulas.

Keywords—Microwave remote sensing, ultra-wide band remote sensing, unmanned aerial vehicle, log-periodic dipole antenna, reflection coefficient.

I. INTRODUCTION

Radar remote sensing of soil moisture [1], soil conductivity [2], soil surface deformations using radar interferometry methods [3], snow cover thickness and density [4], [5], minefield detection [6], arable layer thickness [7], from small unmanned aerial vehicles (UAVs) with using of ultra-wideband (UWB) radars, antenna aperture synthesis and ground-penetrating radar methods [8] is one of the new promising areas. Mainly, broadband log-periodic dipole antennas (LPDA), Vivaldi or Vivaldi-horn antennas are used as transmitting and receiving antennas on UAVs. LPDA antennas have significant frequency dispersion of transfer

function [9]. This phenomenon distorts a transmitted pulse (side lobes of residual ringing appears) even though the pulse spectrum was limited to the passband of the antenna. Specially designed Vivaldi-horn antennas for lightweight UAVs practically do not have distortion of pulse response. Nowadays Vivaldi-horn antennas are widely used as radar antennas on UAVs [10], despite the larger construction volume and weight in relation to LPDA antenna (with the corresponding bandwidth). At the same time, novel methods for designing LPDA and hardware components, implementing corrective time delay circuits have been developed [9]. These approaches significantly reduce the distortion of the pulse response of LPDA. In this paper, we study the possibility of measuring the absolute value of reflection coefficient from the UAV board using LPDA and a portable vector spectrum analyzer (implementing UWB radar). For this purpose, calibration of the UWB radar transmit-receive feeder path using a reference reflector (metal screen) in free space was carried out. The calibration technique is based on previously developed approaches, which consists in software-defined correction of amplitude and phase-frequency responses of LPDA. In contrast to the approach proposed in [11], in this article, due to the high flight altitude of the UAV, there is no need for additional calibration and refinement of the position of the antenna phase center.

II. CALIBRATION METHOD OF UWB UAV RADAR

Let us briefly describe the LPDA [12] calibration method in the nadir bistatic configuration of remote sensing. Antenna's reflection coefficient, $r(\mathbf{f}, \mathbf{h})$ from antenna reference plane can be derive from S-matrix of two-port linear network [11]:

$$r(\mathbf{f}, \mathbf{h}) = r_0(\mathbf{f}) + \frac{G(\mathbf{f}, \mathbf{h})H(\mathbf{f})}{1 - S_{22}(\mathbf{f})G(\mathbf{f}, \mathbf{h})}. \quad (1)$$

Here $r_0(\mathbf{f})$ is the antenna return loss (free space), f is the wave frequency, $H(\mathbf{f})$ is the complex antenna response function (CARF), S_{22} is the antenna backscattering return loss from the side of main lobe, $G(\mathbf{f}, \mathbf{h})$ is the Green's function:

$$G(\mathbf{f}, \mathbf{h}) = R(\mathbf{f})g(\mathbf{f}, \mathbf{h}), \quad (2)$$

$$g(\mathbf{f}, \mathbf{h}) = \exp[2\pi i \frac{f}{c} 2h] / 2h.$$

The investigation supported by the Russian Science Foundation and the Krasnoyarsk Regional Science Foundation, project № 22-17-20042.

Here $R(f)$ is the reflection coefficient from half-space, c is the velocity of light in vacuum. In contrast to the approach in [11], [12], here we will assume that the phase center of the antenna coincides with the geometric center of LPDA. This approximation is appropriate if the phase center of antenna is located at a large distance (compared to the wavelength) from the reflecting plane. Height, large and small bases of trapezoid LPDA are 233mm, 285mm and 95mm, respectively. It is suggested that $S_{22}=0$. Furthermore, assume that antenna's reflection coefficients $\mathbf{r}_m = \mathbf{r}(f, \mathbf{h}_m)$ and $\mathbf{r}_n = \mathbf{r}(f, \mathbf{h}_n)$ can be measured at heights of h_m and h_n , over smooth metal sheet, where $m=1, \dots, P$, $n=1, \dots, P$ ($m \neq n$), P is the total number of heights. Then, from the reduced ratio of antenna's reflection coefficients:

$$\alpha_{nm} \equiv \frac{r(f, h_n) - r_0(f)}{r(f, h_m) - r_0(f)} = \frac{h_m}{h_n} \exp[4\pi i f (h_n - h_m)/c], \quad (3)$$

the estimation of the antenna's reflection coefficient in empty-room $r_0 = r(f, h \rightarrow \infty)$ can be obtained:

$$r_0(f, h_n, h_m) = \frac{r(f, h_n) - \alpha_{nm} r(f, h_m)}{1 - \alpha_{nm}}. \quad (4)$$

From the difference of antenna's reflection coefficients $\mathbf{r}(f, \mathbf{h}_n)$ and $\mathbf{r}(f, \mathbf{h}_m)$, the estimation of CATF can be obtained:

$$H(f, h_n, h_m) = -\frac{r(f, h_n) - r(f, h_m)}{\frac{\exp(2ik_0 h_n)}{2h_n} - \frac{\exp(2ik_0 h_m)}{2h_m}}. \quad (5)$$

Equations (4) and (5) make it possible to determine the spectrum of return loss (in empty room) and CARF from two measurements of antenna's reflection coefficients at any two different heights h_m and h_n of antenna. Finally, $r_0(f)$ and $H(f)$ can be estimated as averaged values of:

$$\langle r_0(f) \rangle = \frac{1}{C_p^2} \sum_{n \neq m} r_0(f, h_n, h_m), \quad (6)$$

where $C_p^2 = P!/(2!(P-2)!)$ is the number combinations without repetition of P elements taken in groups of two elements; $\langle r_0(f) \rangle$ and $\langle H(f) \rangle$ are the average return loss (in empty room) and CATF, calculated for all possible combinations (without repetition) of different antenna heights. As a result of the performed calibration, based on model (1)-(6), it is possible to calculate the modulus of the reflection coefficient from a spatially extended reflector, knowing the flight altitude of the UAV:

$$\frac{R(f)}{2h} = \left| \frac{r(f, h) - \langle r_0(f) \rangle}{\langle H(f) \rangle} \right|. \quad (7)$$

III. RESULT AND DISCUSSION

A. Calibration of UWB UAV Radar

The UAV UWB radar was assembled using a CABAN R60 portable reflectometer manufactured by Planar LLC (Chelyabinsk, the Russian Federation) [13] and LPDA with a bandwidth of 425-1010 MHz. The radar was placed on a quadcopter (Tarot 650 frame) equipped with a LIDAR-Lite v3 laser rangefinder (measurement error ± 1 cm). The software-controlled flight of the UAV was provided by the Pixhawk 4 flight controller and the Intel Computer Stick microcomputer. The developed software (based on python,

MAVLink MAVSDK [14]) allows to synchronize the UAV flight and CABAN R60 reflectometric measurements. The CABAN R60 vector network analyzer was controlled programmatically (Python) using SCPI (Standard Commands for Programmable Instruments) text commands via TCP/IP protocol (STREAM socket). The jMAVSim simulator [15] was used to verify all algorithms for the operation of the equipment and flight tasks. The calibration of the antenna-feeder path of the UWB UAV radar was carried out in free space an open area of yard (55.987979°N, 92.761346°E). Combined sheets of brass mesh were used as a reference metal reflector. The total size of the reference metal screen was 6x7m (Fig. 1). Brass mesh sheets were smoothed, however, individual surface irregularities could reach up to 1.5 cm relative to the level of the asphalt (which also had small vertical irregularities).



Fig. 1. Appearance view of the experimental test site.

In accordance with the previously developed technique, measurements of $r(f, h)$ for calibration of UWB radar antenna-feeder path were carried out from UAV platform hovering at various heights above the brass mesh sheet reflector, approximately from $h=0.8$ m to $h=6$ m. Heights h were measured by an onboard laser rangefinder LIDAR-Lite v3 (calibration plane, which was located at 15 cm above the bottom of the antenna). At each height, the measurements were performed 5 times. Two separate calibration flights were performed. The retrieved values of $r_0(f)$, $H(f)$ are shown in Fig. 2.

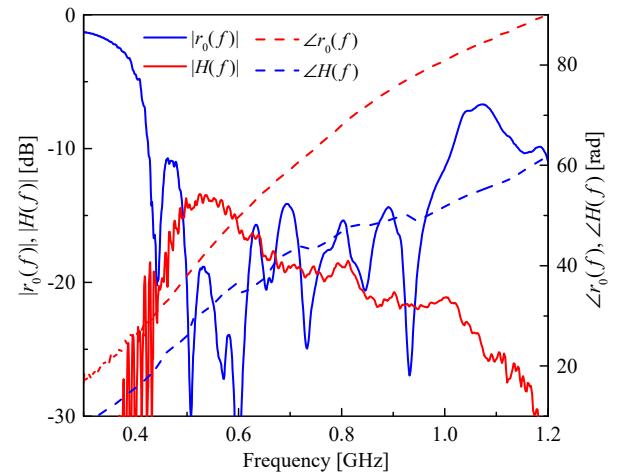


Fig. 2. Measured antenna return loss $r_0(f)$ and complex antenna response function $H(f)$.

B. Error of UWB UAV Radar

In the case of an ideal calibration of the functions $r_0(f)$ and $H(f)$, the left and right parts of equation (7) linearly depends on each other with factor of $1/(2h)$. The measured values of $R(f)/2h$ over brass mesh sheet at three frequencies 500 MHz, 700 MHz, 900 MHz with 5 runs at each height for two separate flights are shown in Fig. 3.

As evident from Fig. 3, measurements of the function $R(f)/2h$, performed at a height of about 0.8 m, for the most part do not lie on the general linear dependence. This effect stems from the use of a simplified model (1), which does not take into account the influence of the near zone of the antenna, as well as the reflection of waves between the UAV elements and the calibration screen. At altitudes higher than 1m, the measurement of $R(f)/2h$ values at individual frequencies is randomly from run to run and from one flight to another within $RMSE=0.017$ 1/m and a determination coefficient of 0.967 (see Fig. 3). This randomly measurement instability (dispersion) can be explained by random re-reflection of the wave over the entire frequency range between the antenna and four rotating propellers. In addition, television stations broadcast in the antenna bandwidth range, as well as telemetry (433 MHz).

The hovering height of the UAV above the brass mesh sheet, measured by the laser rangefinder, correlates well (determination coefficient is 0.999) with the propagation time, t , of the UWB pulse measured by the radar (see Fig. 4). At $t=0$ ns, the hovering height of the UAV is 2.9cm (see caption in Fig. 4), which is close to the value of $RMSE=3.5$ cm. These values of the established errors are within the range measurement error of LIDAR-Lite v3 (± 1 cm) and the brass mesh sheet surface irregularities (up to 1.5 cm).

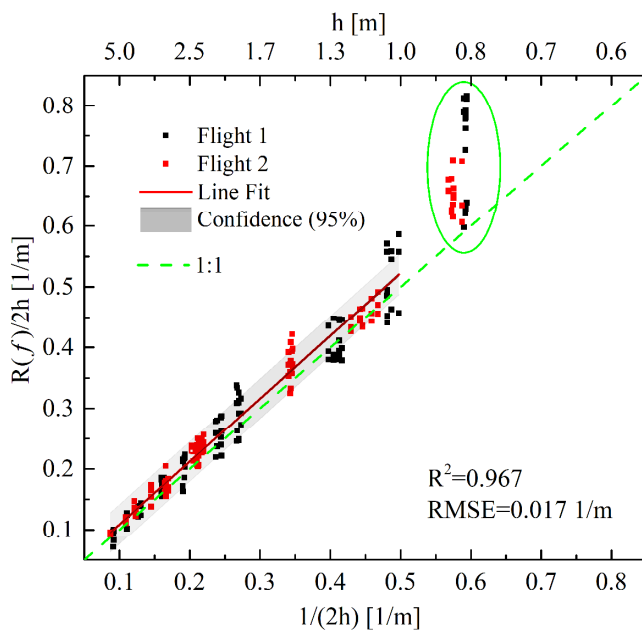


Fig. 3. Dependence of the normalized reflection coefficient on the inverse doubled height of UAV hovering. Linear fitting equation: $R(f)/2h=0.005+1.035/2h$.

As a result of the calibration of the UWB radar based on model (1), it becomes possible to quantitatively measure the modulus of the reflection coefficient and the flight altitude of the UAV. It should be note, in model (1) there are no

restrictions on the analytical representation of the reflection coefficient $R(f)$, e.g. layered structure or presence of any heterogeneities in bottom half-space.

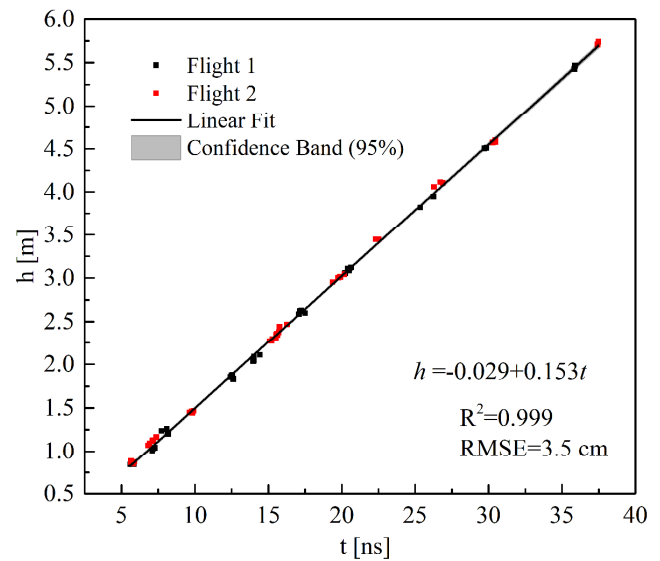


Fig. 4. Correlation between UAV hovering height and impulse propagation delay time. The impulse was calculated from the complex value of $R(f)/2h$ function using the Fourier transform. Red and black dots mark measurements in two different UAV flights.

C. Measure Reflection Coefficient off Lake Water

In order to establish the absolute error in the measurement of reflection coefficient, after the calibration of the antenna-feeder path, the antenna's reflection coefficients $r(f)$ were measured by means of the UWB UAV radar at different hovering heights over a freshwater lake (56.070901°N, 92.708475°E) in the area of the Minino village, Krasnoyarsk Territory, Russia (see Fig. 5).

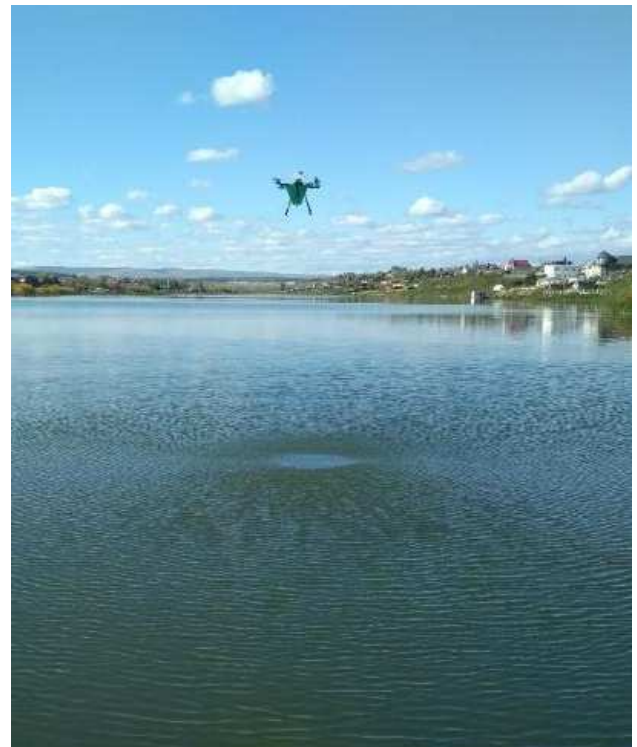


Fig. 5. Photo was taken during the measurement of reflection coefficient off lake water surface by UAV UWB radar.

Measured at the frequencies of 500 MHz, 700 MHz, 900 MHz the reflection coefficient off the lake surface is shown in Fig. 6. At each height, the measurements were carried out 5 times. Fig 6 shows noticeable dispersion (RMSE=0.03-0.05) of measured reflection coefficient $R(f)$. Near the boundaries of the antenna bandwidth (500 MHz, 900 MHz), the measurement error of the reflection coefficient increases (see Fig. 6). Taking into account the correction (see the calibration formula in the caption to Fig. 3), the measured average values of the reflection coefficient at three frequencies (0.77-0.81, see Fig. 6) appeared to be equal to 0.74-0.78. These values are close to the reflection value of 0.799, calculated on the basis of the Stogryn's dielectric model [16] (at a temperature of 20°C and salinity of 0‰), also considering that the real water surface had a random roughness (which reduces the reflection coefficient).

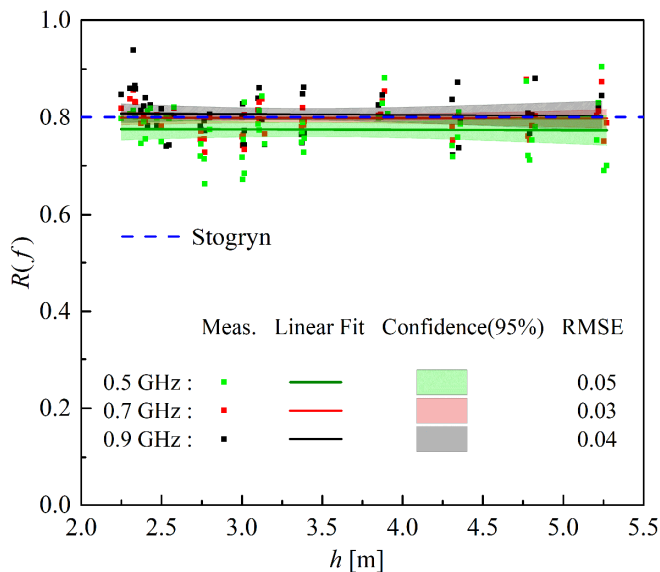


Fig. 6. Measured values of the reflection coefficient off lake water at three frequencies 500 MHz, 700 MHz, 900 MHz. The colors of the dots indicate the measurement frequencies. The colored areas indicate the confidence interval of 95% (five measurements were made at each of the UAV hovering heights).

IV. CONCLUSION

In this work, the calibration errors of the UWB radar transmitting-receiving path equipped with a log-periodic antenna (bandwidth of 425-1010 MHz at -10 dB level) on the UAV platform were investigated. Calibration of the transmitting-receiving path of the UWB UAV radar was carried out by measuring the reflection coefficient in free space from a brass mesh sheets at different hovering heights of the UAV. It is shown that the amplitude of the reflected wave from brass mesh sheets can be measured with root-mean square error (RMSE), $RMSE=0.017$ 1/m and a determination coefficient (R^2) of $R^2=0.967$. Therewith the UAV hovering heights measured by the pulse method and the on-board laser rangefinder correlate with each other with $R^2=0.999$ and with an error of $RMSE=3.5$ cm (measurement error of the laser rangefinder is ± 1 cm, surface irregularities of the brass mesh were no more than 1.5cm). Measured in the frequency range from 500 MHz to 900 MHz, the reflection coefficient from fresh lake water by UAV UWB radar with a relative error of no more than 7.5% coincides with the calculated one

(according to Stogryn's formulas) and practically does not depend on the height of the UAV hovering (approximately from 2.2 to 5.2 m). The proposed method can be implemented to measure reflection coefficient off natural environments with using UAV board.

REFERENCES

- [1] K. Wu, G. A. Rodriguez, M. Zajc, E. Jacquemin, M. Clément, A. De Coster, S. Lambot, "A new drone-borne GPR for soil moisture mapping," *Remote Sensing of Environment*, vol. 235 (111456), p. 1–9, 2019, 10.1016/j.rse.2019.111456.
- [2] K. Wu et al., "Low-Frequency Drone-Borne GPR for Soil Conductivity Mapping," *NSG2021 27th European Meeting of Environmental and Engineering Geo-physics*, p.1 – 5, 2021. doi:10.3997/2214-4609.202120117
- [3] D. Luebeck et al., "Drone-borne Differential SAR Interferometry," *Remote Sensing*, V. 12(5), P. 778, 2020. doi:10.3390/rs12050778
- [4] R.O.R. Jenssen et al., "Measurement of Snow Water Equivalent Using Drone-Mounted Ultra-Wide-Band Radar," *Remote Sens.*, v. 13, p. 2610, 2021. doi:10.3390/rs13132610
- [5] K.V. Myzalevskiy, "The remote sensing of snow water equivalent using broadband electromagnetic pulses from an UAV board," *Zhurnal Radioelektroniki [Journal of Radio Electronics]*, no.8, 2021. doi:10.30898/1684-1719.2021.8.1
- [6] D. Šipoš et al., "A Lightweight and Low-Power UAV-Borne Ground Penetrating Radar Design for Landmine Detection," *Sensors*, v. 20(8), p. 2234, 2020. doi:10.3390/s20082234
- [7] J. Hou et al., "Application of Technology of UAV-Mounted Ground Penetrating Radar in the Study of the Thickness of Soil Plow Layer," *The 7th International Conference on Environmental Science and Civil Engineering*. IOP Conf. Series: Earth and Environmental Science, 2021. doi:10.1088/1755-1315/719/4/042074
- [8] M. ScharTEL, et al, "UAV-Based Ground Penetrating Synthetic Aperture Radar," *IEEE MTT-S Int. Conf. on Micr. for Intel. Mob.* 15-17 April 2018. Munich, Germany, p. 1-4. doi: 10.1109/ICMIM.2018.8443503
- [9] A. Khaleghi, H. S. Farahani and I. Balasingham, "Impulse Radiating Log-Periodic Dipole Array Antenna Using Time-Reversal Technique," *IEEE Antennas and Wireless Propagation Letters*, vol. 10, pp. 967-970, 2011, 10.1109/LAWP.2011.2167735.
- [10] R. Burr, M. ScharTEL, W. Mayer, T. Walter and C. Waldschmidt, "Lightweight Broadband Antennas for UAV based GPR Sensors," *15th European Radar Conference*, Madrid 2018, pp. 245-248, 10.23919/EuRAD.2018.8546552.
- [11] S. Lambot, E. C. Slob, I. van den Bosch, B. Stockbroeckx, M. Vanclooster, "Modeling of ground-penetrating Radar for accurate characterization of subsurface electric properties," *IEEE Transactions on Geoscience and Remote Sensing*, vol. 42, no. 11, pp. 2555-2568, 2004, 10.1109/TGRS.2004.834800.
- [12] K. Muzalevskiy, M. Mikhaylov and Z. Ruzicka, "Synthesizing of Ultra-Wide Band Impulse by means of a Log-Periodic Dipole Antenna. Case Study for a Radar Stand Experiment," *2022 IEEE International Multi-Conference on Engineering, Computer and Information Sciences (SIBIRCON)*, Yekaterinburg, Russian Federation, pp. 1140-1143, 2022, doi: 10.1109/SIBIRCON56155.2022.10017008.
- [13] Planar R60, Planar, Russia, [Online]. Available: https://www.planarchel.ru/catalog/analizatory_tsepey_vektornye/vektornye_reflektometriy_serii_caban/
- [14] MAVSDK, [Online]. Available: <https://mavsdk.mavlink.io/main/en/index.html>
- [15] jMAVSim with SITL, [Online]. Available: <https://docs.px4.io/main/en/simulation/jmavsim.html#jmavsim-with-sitl>
- [16] A. Stogryn, "Equations for Calculating the Dielectric Constant of Saline Water (Correspondence)," *IEEE Transactions on Microwave Theory and Techniques*, vol. 19, no. 8, pp. 733-736, 1971, doi: 10.1109/TMTT.1971.1127617.